Materials Science and Engineering C 48 (2015) 188–196

Contents lists available at ScienceDirect

Materials Science and Engineering C

journal homepage: www.elsevier.com/locate/msec

Mechanical, material, and antimicrobial properties of acrylic bone cement impregnated with silver nanoparticles

Josh Slane [a,*], Juan Vivanco [b,d], Warren Rose [c], Heidi-Lynn Ploeg [b], Matthew Squire [a]

[a] Department of Orthopedics and Rehabilitation, University of Wisconsin–Madison, Madison, WI, USA
[b] Department of Mechanical Engineering, University of Wisconsin-Madison, Madison, WI, USA
[c] School of Pharmacy, University of Wisconsin–Madison, Madison, WI, USA
[d] Facultad de Ingeniería y Ciencias, Universidad Adolfo Ibáñez, Viña del Mar, Chile

ARTICLE INFO

Article history:
Received 24 August 2014
Received in revised form 22 October 2014
Accepted 28 November 2014
Available online 2 December 2014

Keywords:
Bone cement
Infection
Nanoparticles
Antimicrobial
Mechanical properties

ABSTRACT

Prosthetic joint infection is one of the most serious complications that can lead to failure of a total joint replacement. Recently, the rise of multidrug resistant bacteria has substantially reduced the efficacy of antibiotics that are typically incorporated into acrylic bone cement. Silver nanoparticles (AgNPs) are an attractive alternative to traditional antibiotics resulting from their broad-spectrum antimicrobial activity and low bacterial resistance. The purpose of this study, therefore, was to incorporate metallic silver nanoparticles into acrylic bone cement and quantify the effects on the cement's mechanical, material and antimicrobial properties. AgNPs at three loading ratios (0.25, 0.5, and 1.0% wt/wt) were incorporated into a commercial bone cement using a probe sonication technique. The resulting cements demonstrated mechanical and material properties that were not substantially different from the standard cement. Testing against *Staphylococcus aureus* and *Staphylococcus epidermidis* using Kirby-Bauer and time-kill assays demonstrated no antimicrobial activity against planktonic bacteria. In contrast, cements modified with AgNPs significantly reduced biofilm formation on the surface of the cement. These results indicate that AgNP-loaded cement is of high potential for use in primary arthroplasty where prevention of bacterial surface colonization is vital.

1. Introduction

The development of prosthetic joint infection (PJI) is one of the most devastating complications that can arise after total joint arthroplasty. Although the current incidence rates are 2.0 and 2.4% for hip and knee replacement procedures, these values are projected to steadily increase [1]. The development of PJI can cause severe physical and emotional pain to a patient while simultaneously placing a significant burden on the healthcare system in terms of cost and resource allocation. Often times, PJI is attributable to bacterial colonization through biofilm formation on the implant's surface, which makes treatment with traditional systemic antibiotics exceedingly difficult [2]. In response, one of the most common prophylactic techniques against PJI is to incorporate antibiotics into acrylic (PMMA) bone cement to prevent bacterial colonization and proliferation by providing local antibiotic delivery directly at the implant site [3].

The recent rise and spread of multidrug resistant (MDR) microorganisms has become a problem of significant importance worldwide. The widespread use of antibiotics over the past several decades has resulted in the development of genetic and biochemical mechanisms that allow bacteria to survive in antibiotic environments [4]. There has been significant concern over the efficacy of commonly used antibiotics within bone cement, particularly gentamicin, due to the aforementioned rise in MDR microorganisms [5,6]. For example, Hellmark et al. [7] obtained 33 clinical isolates of *Staphylococcus epidermidis* during PJI revision procedures and found a 79% resistance to gentamicin. Similar results were confirmed by Thornes et al. [8] who noted an increased resistance to gentamicin-loaded Palacos bone cement in a rat model. It is generally accepted that while the use of antibiotic-loaded bone cement reduces the possibility of PJI, there is an increase in the possibility of bacterial resistance development [9]. Thus, the problem of reduced antibiotic efficacy has created the need to investigate the potential of incorporating new antimicrobials into bone cement [5].

The use of metallic silver as an antimicrobial agent dates back to antiquity where it was commonly utilized to preserve drinking water and wine [10], however, the development of more potent antibiotics eventually displaced the utility of silver in the clinical setting. The availability of silver nanoparticles (AgNPs) has reopened the use of silver in medical applications since the high surface to volume ratio of nanoparticles imparts unique chemical and physical properties which greatly enhance the antimicrobial effects of silver [11]. Within recent decades, AgNPs have been incorporated into a wide array of consumer and medical products such as fabrics, textiles, plastics, cosmetics, catheters, stents, and wound dressings [12]. Despite this wide usage, the exact mechanism behind the antimicrobial properties of silver is still debated.

* Corresponding author at: 1513 University Ave, Room 3046, Madison, WI 53706, USA.
E-mail address: jaslane@wisc.edu (J. Slane).

http://dx.doi.org/10.1016/j.msec.2014.11.068
0928-4931/

Several mechanisms have been proposed including generation of reactive oxidative species, cationic damage to the bacterial cell membrane, silver–amino acid interaction, and silver–DNA interaction [13]. Regardless of which is correct, one key aspect that makes AgNPs an attractive antimicrobial agent is their well-documented activity against a broad spectrum of microorganisms.

Several previous studies have examined the feasibility of modifying acrylic cements with silver particles for dental and orthopedic applications. For example, Fan et al. incorporated silver benzoate into dental resins and found that the resin exhibited an inhibitory effect against *Streptococcus mutans* [14], however, they noted that silver benzoate concentrations above 0.2% wt/wt inhibited the resin from curing properly. Bone cement modified with silver–tiopronin nanoparticles displayed high antimicrobial efficacy against methicillin resistant *Staphylococcus aureus* [15]. Similar findings were observed by Alt et al. using bone cement loaded with silver nanoparticles against strains of methicillin-resistant *S. epidermidis and S. aureus* [16]. Contrasting results have also been found, most notably by Moojen et al. who reported that metallic silver in bone cement did not prevent methicillin-sensitive Staphylococcal infections in a rabbit model [17]. It is important to note that their study did not examine the cement's ability to prevent bacterial colonization, rather only the antimicrobial effect against planktonic bacteria distant from the embedded metallic silver. They speculated that since metallic silver nanoparticles must be ionized before possessing activity, the antimicrobial effect is delayed and primarily a localized effect that protects the cement surface from bacterial colonization [17]. This is an important characteristic of bone cement modified with silver nanoparticles since PMMA is very susceptible to bacterial adhesion and colonization [18], which is the first stage in the biofilm formation.

While previous studies have investigated various acrylics modified with silver nanoparticles, much of the previous work is limited in scope since many important mechanical and material properties have not been examined. Additionally, many of the techniques used to incorporate silver nanoparticles into acrylic cement utilize techniques that would be difficult to implement in a clinical setting, thus limiting their usefulness. Therefore, the purpose of this study was to modify a commercially available acrylic bone cement with various loadings of silver nanoparticles using a simplistic probe sonication technique. The resulting impact on the cement's mechanical properties, material properties, antimicrobial efficacy, biofilm inhibition and biocompatibility was quantified.

2. Materials and methods

2.1. Cement preparation

A commercially available poly(methyl methacrylate) bone cement, Palacos R (Heraeus Medical GmbH, Wehrheim, Germany), was used as received for all testing. A single cement unit contained a 40 g powder sachet and a 20 mL monomer ampoule. Silver nanoparticles (US Research Nanomaterials, Houston, TX, USA) had a primary particle diameter of 30–50 nm and were surface functionalized with polyvinylpyrrolidone (0.2% wt/wt). This functionalization was used to aid in particle dispersion and minimize agglomeration. Three loading ratios were examined: 0.25, 0.5 and 1.0% wt/wt (relative to the cement powder). The particles were incorporated into the liquid monomer using an ultrasonic homogenizer equipped with a solid titanium tip (150VT, Biologics Inc., Manassas, VA, USA). The monomer/AgNP mixture was sonicated for 12 min within a jacketed reaction vessel. To mitigate heating, cold water was continuously pumped through the vessel and the homogenizer was operated in a pulsed power mode. Standard Palacos (no AgNPs) was also prepared in the same fashion, to ensure consistency among all groups. The monomer/AgNP mixture and powder were then combined by hand in a polymer mixing bowl for 30 s, spaulated into aluminum molds, and allowed to cure for 30 min.

2.2. Mechanical characterization

2.2.1. Static mechanical testing

Four-point bending, compression and single-edge notched beam fracture toughness testing were conducted using methods we previously described [19]. Following cement polymerization, samples were wet ground to the proper dimensions using 400 grit silicon carbide paper. Samples were then allowed to cure for 48 ± 2 h in laboratory conditions (21 °C, 22% humidity) prior to testing. A minimum of eight, ten, and six samples were used for each testing method, respectively. All testing was conducted with an electromechanical materials testing frame with force and displacement data collected at 100 Hz (Criterion C43.104, MTS Systems, Eden Prairie, MN, USA).

2.2.2. Dynamic mechanical analysis

The viscoelastic properties (storage/loss modulus, tan delta) of the cements were assessed using dynamic mechanical analysis (RSA III, TA Instruments, New Castle, DE, USA). Flat beam samples (3 mm thickness, 9.91 mm width) were subjected to dynamic strain sweeps from 0.0005% to 0.08% at 37 °C using a three-point bending configuration with a 40 mm span. Strain was increased logarithmically with 30 points measured per decade. These strains are within the range found within the cement mantle surrounding a femoral prosthesis during the single stance phase of gait [20]. Loading frequencies of 1 and 10 Hz were used and a constant static force of 0.1 N was applied to ensure continuous contact with the bending fixture throughout testing.

2.3. Material characterization

2.3.1. Morphology

The microstructural morphology of the failure surface of four-point bending samples was investigated with scanning electron microscopy (SEM). Samples were mounted on aluminum stubs covered with carbon tape and then sputter coated with gold for 30 s at 45 mA. Images were obtained with a LEO DSM 1530 field emission SEM (Zeiss-LEO, Oberkochen, Germany) using an acceleration voltage of 5 kV and a 5 mm working distance.

2.3.2. Chemical analysis

Compositional changes in the cement caused by the inclusion of AgNPs were monitored with Fourier transform infrared spectroscopy (Equinox 55, Bruker, Billerica, MA, USA) between 4000 and 750 cm^{-1} at a resolution of 2 cm^{-1}. Cement cross sections were scanned in attenuated total reflectance mode at three random sections on each sample, with 32 scans taken at each location. All collected data were averaged to obtain one spectra per cement.

2.3.3. Thermal characteristics

The glass transition temperatures, T_g, of the cements were determined with differential scanning calorimetry (Q100, TA Instruments, New Castle, DE, USA). Samples (5–7 mg) were sealed in aluminum pans and subjected to heating/cooling/heating cycles between 10–160 °C at 20 °C/min. The T_g was determined from the second heating cycle using the method described in ASTM D3418 [21].

The thermal degradation properties of the cement composites were investigated with thermogravimetric analysis (Q500, TA Instruments). Thermograms were obtained from 30–600 °C in a nitrogen environment at a linear heating rate of 20 °C/min. The initial and midpoint decomposition temperatures were determined, which are the points where 10% and 50% of the material had decomposed, respectively.

2.3.4. Elemental composition

The presence of AgNPs in the cements was confirmed using X-ray photoelectron spectroscopy (K-Alpha XPS, Thermo Scientific, Waltham, MA, USA). Thin cross-sections (~2 mm) were taken from cement beams with a water-irrigated slow speed diamond saw. Initial survey spectra

Table 1
Results (mean ± SD) obtained from static mechanical testing. All cements exceed the benchmarks set in ISO 5833.

Sample	Flexural modulus (MPa)	Flexural strength (MPa)	Yield strength (MPa)	Compressive modulus (GPa)	Fracture toughness (MPa·√m)	Work-of-fracture (kJ/m$^{2)}$
Palacos R	2961 ± 142	71.5 ± 2.8	104 ± 1	1.85 ± 0.07	1.72 ± 0.11	0.80 ± 0.03
0.25% AgNP	2893 ± 65	69.0 ± 2.9	99 ± 2[a]	1.67 ± 0.12[a]	1.61 ± 0.14	0.64 ± 0.03[a]
0.5% AgNP	2907 ± 105	69.1 ± 2.6	98 ± 3[a]	1.74 ± 0.06[a]	1.60 ± 0.11	0.65 ± 0.03[a]
1% AgNP	2960 ± 161	68.8 ± 4.7	100 ± 1[a]	1.71 ± 0.06[a]	1.66 ± 0.07	0.60 ± 0.02[a]

[a] $p < 0.05$, relative to standard Palacos R.

were acquired within a randomly chosen 400 μm region at a constant pass energy of 200 eV from binding energies of 0 to 1350 eV with a step size of 1 eV. Based on the survey spectra, regions of interest were identified and high-resolution scans were obtained using a 50 eV pass energy and step size of 0.1 eV.

2.3.5. Biocompatibility

A transgenic mouse osteoblast cell line (TMOb) was used to assess the biocompatibility of the cements. TMOb cells were cultured to confluence in growth medium containing minimum essential medium (MEM) alpha, 10% fetal bovine serum, and 1% penicillin–streptomycin (Invitrogen, Carlsbad, CA, USA) at 37 °C with 5% CO_2. Cells were harvested using TrypLE Select (Invitrogen) and pooled in 15 mL of growth medium. 0.1 mL of cell suspension/well was added to 6-well plates containing 2 mL of non-mineralization medium. Cells were grown to confluence and cement disks (6 mm diameter, 2 mm thickness) were placed in the well. Cell viability was assessed after 1 and 3 d using an automated cell counter (Countless, Invitrogen) according to the manufacturers' protocol. Each treatment was assessed in triplicate and all cement samples used were sterilized with ethylene oxide prior to testing. An additional control of the well plate alone without exposure to any cement was also tested.

2.4. Antimicrobial testing

A modified Kirby-Bauer disk diffusion assay was used to determine the inhibitory zone of antimicrobial activity of the cements against *S. epidermidis* and *S. aureus*. A positive control cement containing a 2% wt/wt loading of gentamicin (Palacos R + G) was also tested. Six bacterial isolates were used: two controls (*S. aureus* ATCC 29213 and *S. epidermidis* ATCC 35984) and four clinical isolates (CI) obtained from patients with active joint infections (two *S. aureus* and two *S. epidermidis*). The bacteria were incubated on Mueller-Hinton agar (MHa) for 18 to 24 h at 37 °C. Colonies were then suspended in saline to a 0.5 McFarland standard turbidity measurement. An inoculum of ~10^6 CFU/mL was obtained by spreading 200 μL of the suspension onto MHa plates. Cement disks (6 mm diameter, 2 mm thickness) were placed on top of the MHa plates and incubated for 18 to 24 h at 37 °C. The resulting zone of inhibition (area of no bacterial colony growth) was measured and compared to the negative control cements.

Time-kill assays against planktonic cells were performed using two isolates: one clinical methicillin-resistant *S. aureus* (MRSA) isolate collected from a patient with PJI and one control strain of *S. epidermidis* (ATCC 35984). Bacterial cultures were maintained in Mueller-Hinton broth supplemented with 25 mg/L calcium and 12.5 mg/L magnesium. A starting inoculum of 5×10^5 CFU/mL (colony forming units) was obtained in culture from a 100-fold dilution of a 0.5 McFarland standard measured using a densitometer. Each experiment was conducted in a total volume of 2 mL of media in 24 well TPP tissue culture-treated plates (Sigma-Aldrich, St. Louis, MO, USA). Cement disks (6 mm diameter, 2 mm thickness) were placed into the 2 mL well culture containing the test organism at the standardized inoculum and incubated with shaking at 80 rpm at 35 °C. 0.1 mL aliquots were removed from the cultures at 0, 2, 4, and 8 h and were serially diluted in cold 0.9% NaCl. Bacterial counts were determined by spot plating 20 mL aliquots of time samples on Mueller-Hinton agar and manually counting bacterial colonies to determine CFU/mL after 18–24 h of incubation at 35 °C.

The ability of the cements to prevent biofilm formation was evaluated in a modified adhesion culture assay using the same strains as in the time-kill assays. All studies were performed in Tryptic soy broth supplemented with 1% glucose to facilitate rapid biofilm development [22]. To evaluate prevention of biofilm formation, the disks were placed in a

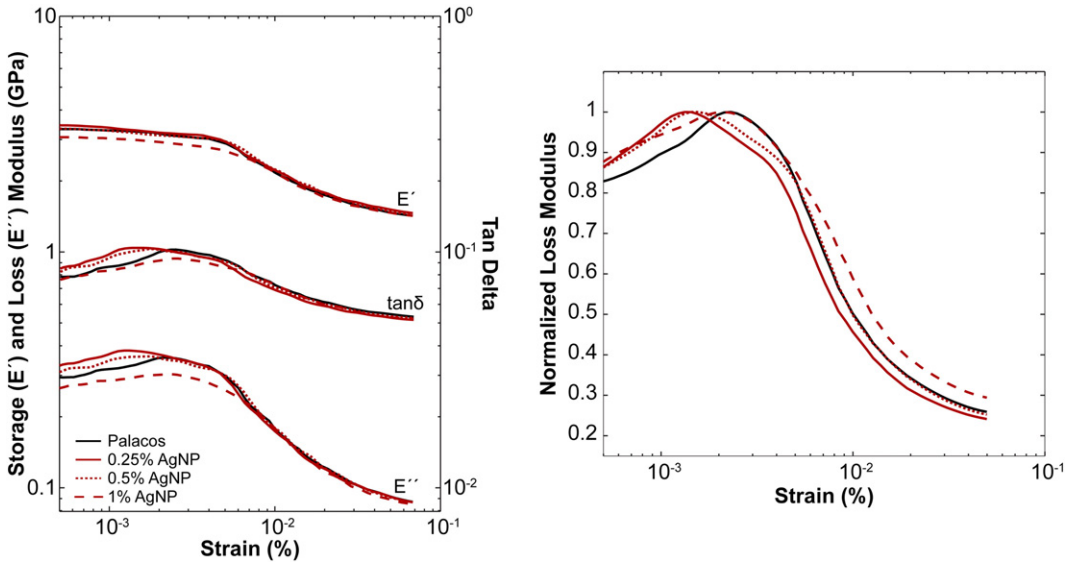

Fig. 1. Left — Results from DMA strain sweeps. Only data from 1 Hz is shown, for clarity purposes. At a loading frequency of 10 Hz, similar profiles for all cements were observed, however, the relative magnitudes were increased. Right — Normalized loss modulus curves (E″/E″max) for cements at a loading frequency of 1 Hz. The legend is applicable to both curves.

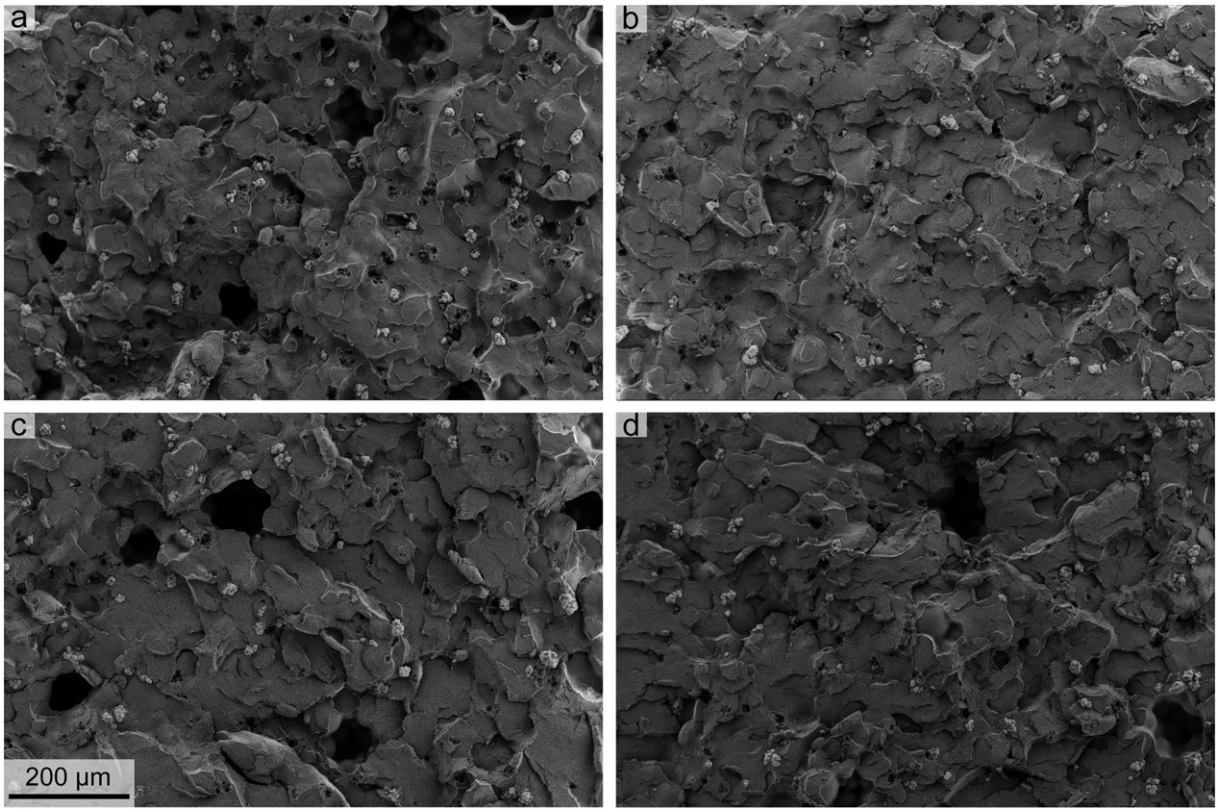

Fig. 2. Representative scanning electron micrographs at 300× of the failure surface of four point bending samples. The scale bar is applicable to all images. a) Palacos, b) 0.25% AgNP, c) 0.5% AgNP, and d) 1% AgNP.

bacterial culture of 5×10^5 CFU/mL obtained as described previously and allowed to co-incubate at 35 °C for 24 h with agitation at 120 rpm. The disk and medium were carefully removed and the wells were gently washed with 1 mL of a 1 × PBS solution three times without disrupting the biofilm adhesion on the well bottom. The biofilm was dried and fixed to the bottom of the plate by heat incubation at 60 °C for 1 h. The biofilm was then stained with 1 mL of a 1% crystal violet solution, and the residual stain was removed with deionized water. Plates were air-dried and the optical density at 570 nm (OD_{570}) of the stained adherent bacterial films was measured [23]. For all antimicrobial assays, testing was performed in triplicate and cement samples were sterilized with ethylene oxide (EtO) prior to testing.

2.5. Statistics

Statistical analysis was performed using Minitab 15 (Minitab Inc., State College, PA) with a significance level of 5% set for all tests. Normality of the mechanical testing data was first confirmed using the Kolmogorov–Smirnov method and data were therefore analyzed using a one-way analysis of variance (ANOVA) with Tukey's HSD post-hoc

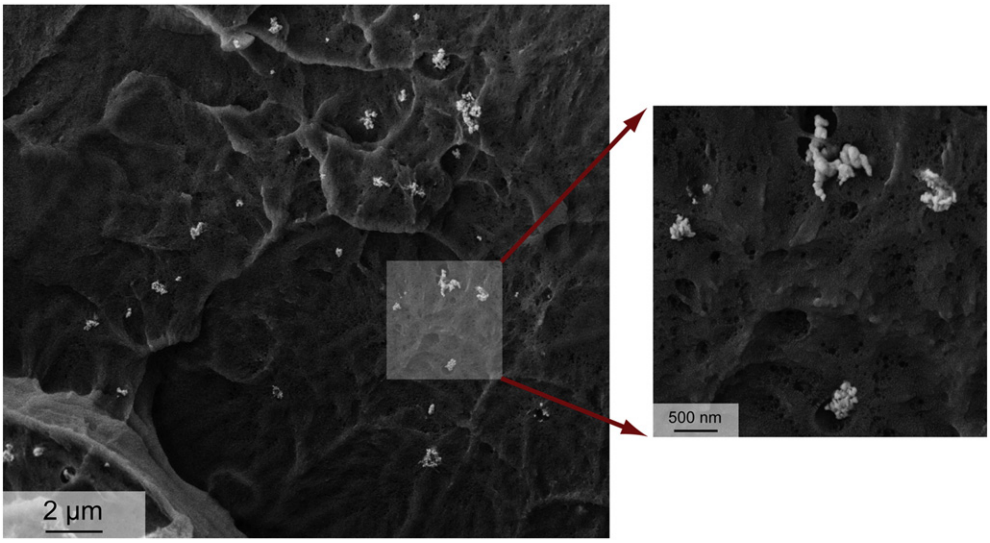

Fig. 3. SEM image taken at 10 kx (insert at 50 kx) showing small agglomerations of AgNPs.

analysis. All other collected data were analyzed using the same method. Where applicable, data are presented as the mean ± standard deviation.

3. Results

3.1. Mechanical characterization

3.1.1. Static mechanical testing

Standards for the flexural and compressive properties of acrylic bone cement are established in ISO 5833 [24]. According to this standard, cements must possess a flexural strength, flexural modulus and compressive strength of 50 MPa, 1800 MPa, and 70 MPa, respectively. All cements tested in this study easily surpassed these requirements. Flexural properties were not influenced by the addition of AgNPs (Table 1). While both the flexural modulus and strength tended to slightly decrease with higher AgNP concentration, these results were not significant. Yield strength and compressive modulus both significantly decreased with the addition of AgNPs. For yield strength, the largest percent decrease was observed for the 0.5% loading (5.8%) while for modulus the 0.25% loading (9.7%). Fracture toughness was not significantly influenced by particle addition, however, work-of-fracture significantly decreased with increasing AgNP concentration.

3.1.2. Dynamic mechanical analysis

The storage modulus (E′), loss modulus (E″) and tan delta (tanδ) of the cements are shown in Fig. 1. Similar magnitudes in storage modulus were observed for all cements, with 1% AgNP being slightly lower than others. The storage modulus profiles were consistent for all cements except 1% AgNP, which exhibited a broadened slope and began to decrease after the other cements. More prominent differences were observed in the loss modulus of the cements, which differed in magnitude and profile, and cement containing 1% AgNP had the largest deviation from Palacos. The value of tanδ was consistent among cements, however, the peak location of tanδ occurred at slightly different strain levels. Testing frequency was found to have an impact on the resulting viscoelastic properties, as expected. With increased frequency, the profiles of all properties stayed consistent with those observed at 1 Hz but the relative magnitudes increased.

The impact of AgNP addition on the properties of the cements was demonstrated by normalizing the loss modulus curves, as shown in Fig. 1. For 0.25% and 0.5% AgNPs, the resulting E''/E''_{max} curve is essentially a pure horizontal shift, relative to standard Palacos. In contrast, for 1% AgNP, the curve is broadened and higher in magnitude at larger strains. This slight change in viscoelastic response could result from polymer chain immobilization by the AgNPs and secondary interactions between the polymer and particle [25].

3.2. Material properties

3.2.1. Morphology

Analysis of the fracture surface of four-point bending samples with scanning electron microscopy revealed no apparent differences, indicating that the addition of AgNPs did not alter the failure mechanism of the standard cement (Fig. 2). The sonication technique used to incorporate the AgNPs within the cement resulted in a relatively homogeneous dispersion of particles. AgNPs were observed to agglomerate within the cement, however, even the largest of these agglomerations were under 1 μm in size (Fig. 3).

3.2.2. Chemical analysis

Collected FTIR spectra displayed characteristic peaks for acrylic bone cement, as expected (Fig. 4). The most prominent peaks occurred at 1730 cm^{-1} and 1140 cm^{-1} which correspond to a C═O stretch and O – C – C stretch, respectively. Analysis of the collected FTIR spectra showed no differences in the position or magnitude of intensity peaks between the different cements, indicating that there was no formation of new chemical groups.

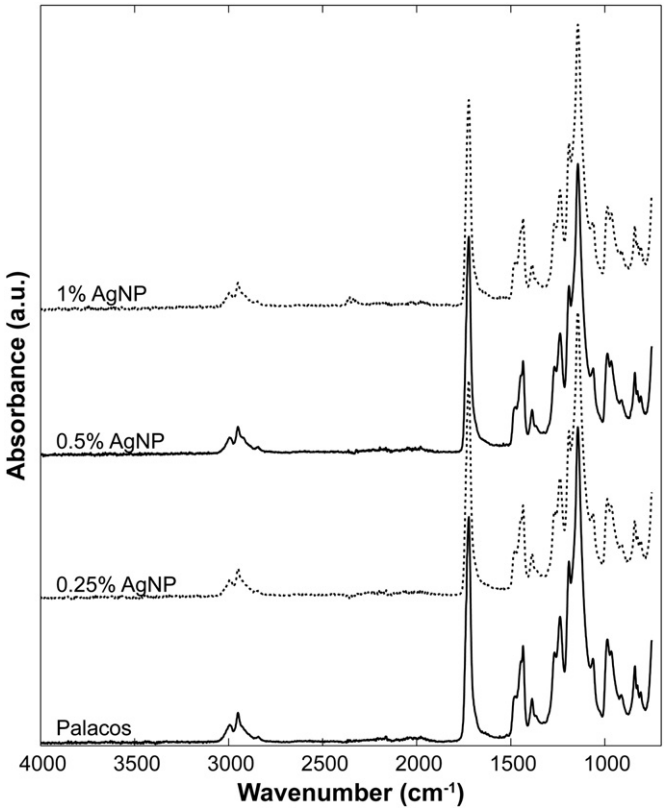

Fig. 4. Collected ATR-FTIR spectra for each cement. Each curve is an average of 96 individual measurements. The slight peak seen for 1% AgNP at ~2400 cm^{-1} is attributable to atmospheric CO_2 and is not indicative of the material.

3.2.3. Thermal characteristics

The addition of silver nanoparticles had no significant influence on the glass transition temperature of the cements (Table 2). The initial decomposition temperature decreased with increasing AgNP concentration. This finding likely results from the degradation of the polyvinylpyrrolidone coating on the silver nanoparticles. The midpoint decomposition temperatures were slightly different between cements, but the differences were not as pronounced as the initial decomposition point.

3.2.4. Elemental composition

The elemental composition of the cements determined using X-ray photoelectron spectroscopy was found to consist of carbon, oxygen, silver, and zirconium (the radiopacifier in the cement). High-resolution XPS spectra collected from binding energies of 360 to 380 eV showed an increase in peak intensities with increasing AgNP content, as expected (Fig. 5).

Table 2
The glass transition (T_g), initial thermal decomposition temperature (T_{10}), and midpoint decomposition (T_{50}) obtained from TGA and DSC testing.

Sample	T_g (°C)	T_{10} (°C)	T_{50} (°C)
Palacos R	98.5 ± 0.6	337.8	382.2
0.25% AgNP	98.0 ± 0.7	329.0	380.5
0.5% AgNP	97.2 ± 0.7	327.6	379.9
1% AgNP	97.6 ± 0.6	323.6	377.6

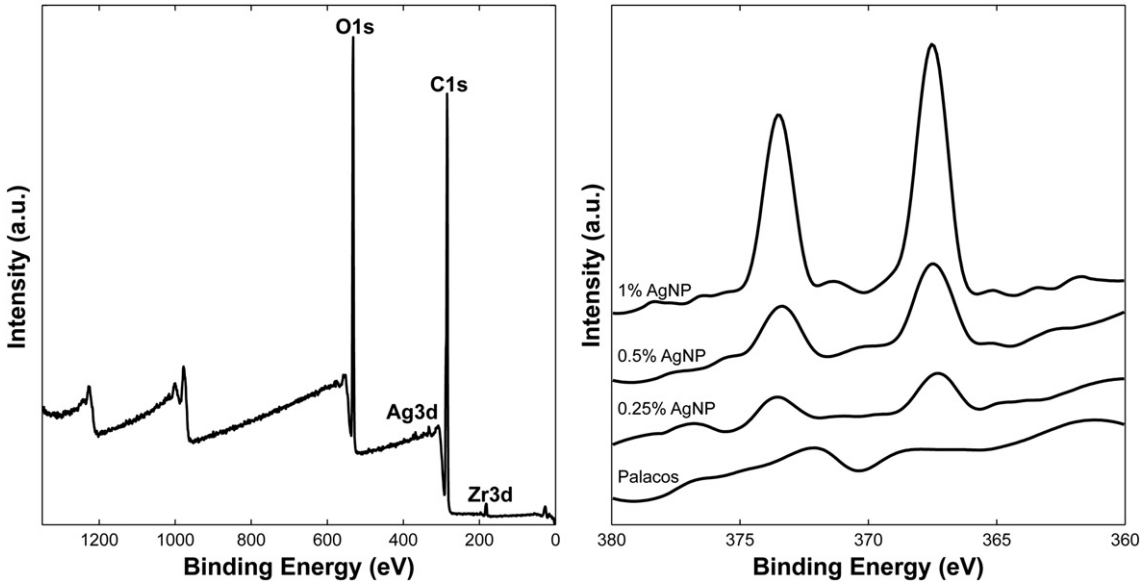

Fig. 5. XPS spectra of the cements. Left — XPS survey spectra, right — high-resolution XPS spectra of Ag3d.

3.2.5. Biocompatibility

The viability of TMOb cells was assessed following exposure to cement disks for 1 and 3 d. It was found that cement exposure, regardless of AgNP content, had no significant effect on the viability of the osteoblast cells. This result was consistent for both 1 and 3 d.

3.3. Antimicrobial testing

Results obtained from the Kirby-Bauer assays demonstrated that plain Palacos and cements modified with AgNPs had no antimicrobial activity (Table 3). In contrast, the positive control (cement with gentamicin) exhibited large zones of inhibition for all bacterial strains tested. Interestingly, small colony variants were found within the zone of inhibition for a clinical isolate of *S. epidermidis* (Fig. 6). These colonies were further tested for specific susceptibility to gentamicin and the minimum inhibitory concentration exceeded 32 mg/L, indicating heteroresistance to gentamicin. Similar results were also confirmed in the time-kill studies; AgNP-loaded cement had no antimicrobial effect on planktonic bacteria (Fig. 7a and b). In contrast, biofilm formation was significantly influenced ($p < 0.001$) by the presence of AgNPs within the bone cement. For both tested strains, cement containing 0.5% AgNP resulted in the highest biofilm inhibition for *S. epidermidis* and *S. aureus*, respectively (Fig. 7c and d) however these results were not always significant relative to the other AgNP loading ratios.

4. Discussion

The use of antibiotic-loaded bone cement was first popularized in the early 1970s by Buchholz and Engelbrecht, who added lyophilized gentamicin to Palacos bone cement [26]. Since that time, gentamicin has become one of the most common antibiotics used in both surgeon-prepared and commercially available antibiotic-loaded bone cements, despite issues pertaining to bacterial resistance. Other antibiotics such as vancomycin and tobramycin are also frequently used in bone cement, especially in revision procedures, but again reports of resistance have emerged thus limiting their effectiveness [27–29]. Silver nanoparticles are attractive alternatives to conventional antibiotics since it is postulated that microorganisms are unlikely to develop silver-resistance. The wide variety of pharmacological targets of silver implies that bacteria would have to develop multiple phenotypic and genetic mutations simultaneously to be protected from its antimicrobial actions [30].

The formation of biofilm on the surface of an orthopedic implant, which begins with the passive adhesion of bacteria to a surface, is a substantial problem that makes treatment of prosthetic joint infections difficult [31]. For example, the antimicrobial minimum inhibitory concentrations of bacteria encased in biofilm can be 100 to 1000 times higher relative to bacteria in the planktonic (non-adherent) state due to high organism burden, non-replicating, stationary bacterial cells, and poor antimicrobial diffusion in biofilm [32]. Bacterial adhesion testing conducted in this study showed that bone cement containing AgNPs significantly reduced biofilm formation, regardless of the loading ratio of AgNPs. Furthermore, it was found that a loading ratio of 0.5% AgNP resulted in the highest biofilm inhibition levels with reductions of 83.1% and 76.7% for *S. epidermidis* and *S. aureus*, respectively (Fig. 7c and d). These results were not always significantly different from the other loading ratios. In contrast to the biofilm inhibition testing, the Kirby-Bauer and time-kill assays performed in this study demonstrated no antimicrobial activity for AgNP-loaded cements against *S. aureus* and

Table 3
Resulting (mean ± SD) zone of inhibition (mm) from the Kirby-Bauer assays against control and clinical isolate (CI) strains of *S. aureus* and *S. epidermidis*. Palacos R + G contains 2% wt/wt gentamicin premixed into the cement.

Cement	*S. aureus* ATCC 29213	*S. epid* ATCC 35984	*S. aureus* CI-1	*S. aureus* CI-2	*S. epid* CI-1	*S. epid* CI-2
Palacos R	0	0	0	0	0	0
Palacos R + G	27.3 ± 3.4	22.0 ± 7.3	28.8 ± 0.9	20.8 ± 2.8	37.2 ± 1.5[a]	22.9 ± 1.0
0.25% AgNP	0	0	0	0	0	0
0.5% AgNP	0	0	0	0	0	0
1% AgNP	0	0	0	0	0	0

[a] Heteroresistance to gentamicin observed.

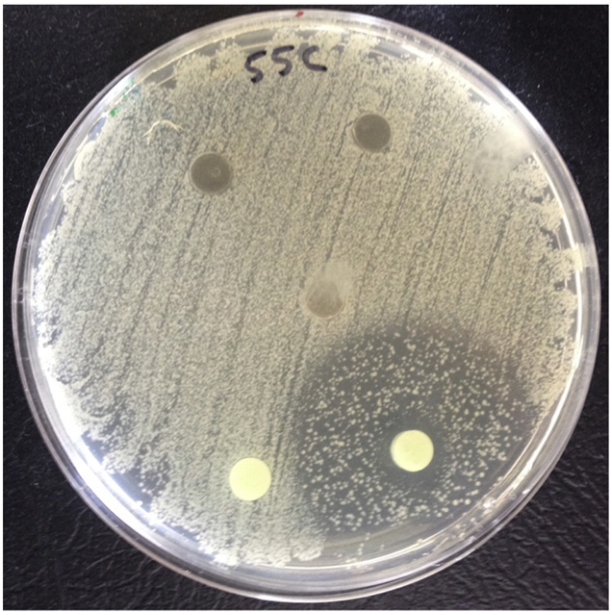

Fig. 6. Representative result from Kirby-Bauer assay testing against a clinical isolate of *S. epidermidis*. The top three black samples contain AgNPs, bottom left is the negative control, and the bottom right contains gentamicin. Small colonies were found within the zone of inhibition, confirmed as heteroresistance to gentamicin when individually tested for susceptibility.

S. epidermidis. Interestingly, the presence of heteroresistance to gentamicin was observed in one of the clinical isolate strains (*S. epidermidis*) tested with the Kirby-Bauer assay (Fig. 6). Heteroresistance refers to the presence of subpopulations of bacteria within the population exhibiting reduced susceptibility to a specific drug [33]. This is of significant clinically importance because a fully resistant population can emerge with antibiotic treatment, which has corresponded to treatment failure [34,35].

Many different types of silver, such as metallic nanoparticles and silver salts, have been used as antimicrobial agents within polymers. One of the earliest examples of use within bone cement was demonstrated by Spadaro et al. who incorporated various silver salts into Simplex P cement and observed a significant antimicrobial activity against *Pseudomonas aeruginosa* and *S. aureus* [36]. Caution must be exercised however when using soluble silver salts since toxicity driven by concentration dependency has been previously demonstrated [37]. For example, serious neurological defects were noted 5 yr post-op in a patient who received a cemented total hip replacement impregnated with ~3% wt/wt silver salt by Sudmann et al. [38].

In contrast to silver salts, insoluble metallic silver nanoparticles like those used in the current study must first be ionized prior to exerting an antimicrobial activity. Upon contact with an AgNP, it is speculated that the bacterial cell uptakes silver ions thus generating reactive oxygen species that evoke an antimicrobial action [30]. Assuming that the particles are entrapped within the polymer matrix and not released into the surrounding fluid, they are theoretically less prone to toxicity issues. This approach was attempted by Moojen et al. who used metallic AgNPs (with aggregates of 2–5 μm) at loading ratios of 0.6 and 1.0% wt/wt to modify Simplex P cement. These cements were implanted into an infected rabbit wound bed model and no antibacterial efficacy was found, however, they did not investigate the biofilm inhibition properties that are more akin to the initial stages of implant infections [17]. Similar results were confirmed in this study through the Kirby-Bauer and time-kill assays. These results suggest that this type of AgNP-impregnated cement is likely unsuitable for situations where an active infection is present, such as use in an exchange arthroplasty. However, the significant biofilm inhibitory properties may be of great use in primary arthroplasties where it is important to prevent initial bacterial colonization of the cement surface.

The two primary roles of bone cement are to provide immediate implant fixation following surgery and to distribute loads from the implant to the surrounding bone bed in order to avoid stress shielding. Therefore, it is vital that additives to the cement do not substantially alter the inherent mechanical properties. In this study, the static mechanical properties were tested following a post-fabrication curing

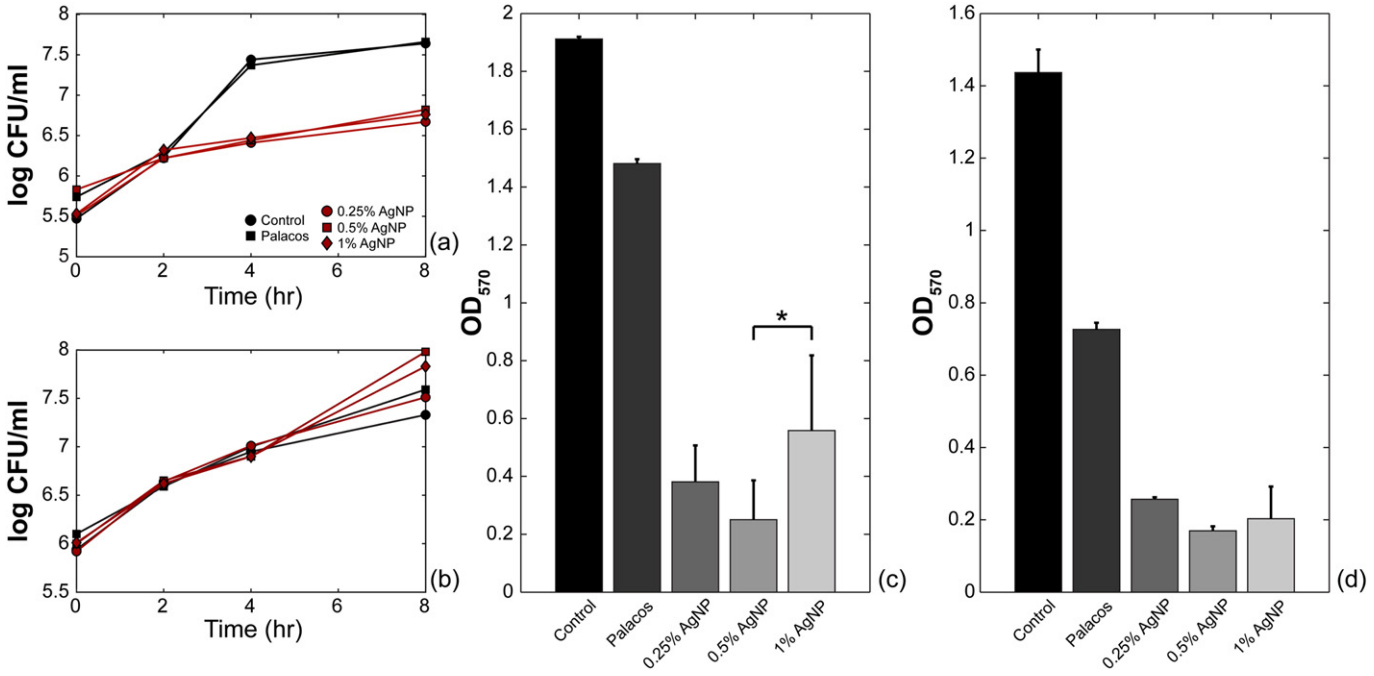

Fig. 7. Results from planktonic time-kill assays on *S. epidermidis* (a) and *S. aureus* (b). AgNP-loaded cement reduced biofilm formation for both *S. epidermidis* (c) and *S. aureus* (d). 'Control' refers to plain tissue culture plastic. All cements containing AgNPs significantly ($p < 0.001$) reduced biofilm relative to the control and Palacos bone cement. An * indicates a significant ($p < 0.05$) difference.

time of 48 ± 2 h, while the ISO standard for bone cement calls for a 24 ± 2 h curing time [24]. Although increasing the curing time after fabrication can enhance the static mechanical properties, the relative change from one to two days is insignificant [39]. Interestingly, the compressive properties of the cements significantly decreased with the addition of AgNPs, yet their values were still considerably above those stipulated in the ISO standard. The work of fracture was significantly decreased with AgNP addition, which could indicate particle/matrix debonding [40]. This could also explain the slight, albeit non-significant, reduction seen in the flexural properties and fracture toughness however more work is needed to determine the exact mechanism.

Since bone cement distributes load to the surrounding bone it must possess mechanical properties that are an intermediary of the prosthesis and bone. DMA testing confirmed that this holds true for all AgNP-loaded cements. At a frequency of 1 Hz and strain of 0.01%, the E′ ranged from 2.09 to 2.2 GPa while tanδ was between 0.07–0.08. These values are in good agreement and are between those of cancellous bone, which has a storage modulus of 0.2 GPa and tanδ of 0.09–0.1 (cortical bone 0.04), and metals typically used for implants which have a storage modulus exceeding 100 GPa and a tanδ of ~10^{-4} [41].

The intrinsic material properties of the Palacos cement were relatively unchanged by the addition of AgNPs. Fourier transform infrared spectroscopy revealed no change in cement composition from the addition of AgNPs and DSC/TGA testing showed no substantial effect on the thermal properties, which is consistent with previously reported thermal characteristics of silver nanocomposites [42,43]. Similarly, as seen in Fig. 2, AgNPs did not alter the morphology of the samples and the apparent failure mechanism was consistent across all groups. The sonication technique used to incorporate the particles within the cement achieved an overall good dispersion within the cement matrix with relatively small particle agglomerations. The cements were found to possess no cytotoxic effects against osteoblast cells and cell viability was not significantly different for any cement type. Care must be taken however when interpreting biocompatibility results since in vitro testing is a substantial simplification of the in vivo scenario. Finally, although not assessed directly, on a qualitative level the handling characteristics (e.g. curing time, apparent viscosity) of the cements were not influenced by the presence of AgNPs, which is an important aspect from a clinical viewpoint.

Several limitations to the current study are recognized. Firstly, only a single cement variety (Palacos R) was used and other types with different chemical formulations and viscosities could elicit different results. This specific cement was chosen because it is one of the most commonly used bone cement formulations worldwide [44]. Secondly, the fatigue properties of the AgNP-loaded cements were not measured although it is well known that fatigue is a major contributor to in vivo cement failure [45]. It was deemed beyond the scope of the current project to perform fatigue testing. Thirdly, only two bacterial strains were used for biofilm testing yet others could respond differently to the cements. The clinical MRSA isolate was collected from an implant infection known to involve large amounts of biofilm formation and represents the increasing problem of multi-drug resistant infections in this setting and the *S. epidermidis* control strain is a well-described high biofilm producing control. Collectively, these two organisms represent the vast majority of causative pathogens in implant infections, and therefore they were deemed highly relevant to evaluate biofilm inhibition. Additionally, the biofilm assay was only conducted over 1 day for practical considerations, but future work should examine the inhibition properties over an extended period to see if they persist. Finally, the biocompatibility testing only measured cell viability even though other markers, such as cell proliferation and lactate dehydrogenase, are of relevance. Future testing should include a more comprehensive analysis of biocompatibility. Despite these limitations, this is the first study to our knowledge to provide a detailed characterization of the mechanical, material, and antimicrobial properties of acrylic cement modified with AgNPs.

5. Conclusion

In this study, it has been shown that acrylic bone cement can be impregnated with low concentrations of metallic silver nanoparticles. The resulting cement composites have mechanical and material properties that are not substantially different from the standard cement. Antimicrobial testing demonstrated that AGNP cements have no antimicrobial activity against planktonic bacteria, however, they were able to significantly reduce the formation of biofilm on the cement's surface. These results imply that AgNP-loaded cements are of high potential use in primary arthroplasties where prevention of bacterial adhesion is required.

Acknowledgments

The authors thank Michael Johnson for his assistance with biocompatibility testing. The authors gratefully acknowledge the use of facilities and instrumentation supported by the NSF-funded University of Wisconsin Materials Research Science and Engineering Center (DMR-1121288). Funding for this project was provided through the University of Wisconsin Innovation & Economic Development Research Program. The sponsor had no involvement in this work.

References

[1] S.M. Kurtz, E. Lau, H. Watson, J.K. Schmier, J. Parvizi, Economic burden of periprosthetic joint infection in the United States, J. Arthroplast. 27 (2012) 61–65 (e1).
[2] A. Trampuz, A.F. Widmer, Infections associated with orthopedic implants, Curr. Opin. Infect. Dis. 19 (2006) 349–356.
[3] J. Meyer, G. Piller, C.A. Spiegel, S. Hetzel, M. Squire, Vacuum-mixing significantly changes antibiotic elution characteristics of commercially available antibiotic-impregnated bone cements, J. Bone Joint Surg. (Am. Vol.) 93 (2011) 2049–2056.
[4] V. Seputiene, J. Povilonis, J. Armalyte, K. Suziedelis, A. Pavilonis, E. Suziedeliene, Tigecycline — how powerful is it in the fight against antibiotic-resistant bacteria? Medicina (Kaunas) 46 (2010) 240–248.
[5] G. Lewis, Viscoelastic properties of injectable bone cements for orthopaedic applications: state-of-the-art review, J. Biomed. Mater. Res. 98 (2011) 171–191.
[6] J. Parvizi, K. Azzam, E. Ghanem, M.S. Austin, R.H. Rothman, Periprosthetic infection due to resistant staphylococci: serious problems on the horizon, Clin. Orthop. Relat. Res. 467 (2009) 1732–1739.
[7] B. Hellmark, M. Unemo, A. Nilsdotter-Augustinsson, B. Soderquist, Antibiotic susceptibility among *Staphylococcus epidermidis* isolated from prosthetic joint infections with special focus on rifampicin and variability of the rpoB gene, Clin. Microbiol. Infect. 15 (2009) 238–244.
[8] B. Thornes, P. Murray, D. Bouchier-Hayes, Development of resistant strains of *Staphylococcus epidermidis* on gentamicin-loaded bone cement in vivo, J. Bone Joint Surg. (Br.) 84 (2002) 758–760.
[9] M. Kyomoto, T. Moro, K. Ishihara, Polymers for artificial joints, in: S. Dumitriu, V. Popa (Eds.), Polymeric Biomaterials: Structure and Function, CRC Press: CRC Press, 2013, pp. 851–883.
[10] X. Chen, H.J. Schluesener, Nanosilver: a nanoproduct in medical application, Toxicol. Lett. 176 (2008) 1–12.
[11] M.K. Rai, S.D. Deshmukh, A.P. Ingle, A.K. Gade, Silver nanoparticles: the powerful nanoweapon against multidrug-resistant bacteria, J. Appl. Microbiol. 112 (2012) 841–852.
[12] M. Pollini, F. Paladini, A. Licciulli, A. Maffezzoli, A. Sannino, Engineering nanostructured silver coatings for antimicrobial applications, in: N. Cioffi, M. Rai (Eds.), Nano-antimicrobials: Progress and Prospects, Springer-Verlag, Berlin, 2012, pp. 313–336.
[13] H. Zhang, M. Wu, A. Sen, Silver nanoparticle antimicrobials and related materials, in: N. Cioffi, M. Rai (Eds.), Nano-antimicrobials: Progress and Prospects, Springer-Verlag, Berlin, 2012, pp. 18–60.
[14] C. Fan, L. Chu, H.R. Rawls, B.K. Norling, H.L. Cardenas, K. Whang, Development of an antimicrobial resin—a pilot study, Dent. Mater. 27 (2011) 322–328.
[15] P. Prokopovich, R. Leech, C.J. Carmalt, I.P. Parkin, S. Perni, A novel bone cement impregnated with silver–tiopronin nanoparticles: its antimicrobial, cytotoxic, and mechanical properties, Int. J. Nanomedicine 8 (2013) 2227–2237.
[16] V. Alt, T. Bechert, P. Steinrucke, M. Wagener, P. Seidel, E. Dingeldein, et al., An in vitro assessment of the antibacterial properties and cytotoxicity of nanoparticulate silver bone cement, Biomaterials 25 (2004) 4383–4391.
[17] D.J. Moojen, H.C. Vogely, A. Fleer, A.J. Verbout, R.M. Castelein, W.J. Dhert, No efficacy of silver bone cement in the prevention of methicillin-sensitive Staphylococcal infections in a rabbit contaminated implant bed model, J. Orthop. Res. 27 (2009) 1002–1007.
[18] E. Bertazzoni Minelli, T. Della Bora, A. Benini, Different microbial biofilm formation on polymethylmethacrylate (PMMA) bone cement loaded with gentamicin and vancomycin, Anaerobe 17 (2011) 380–383.

[19] J. Slane, J. Vivanco, J. Meyer, H. Ploeg, M. Squire, Modification of acrylic bone cement with mesoporous silica nanoparticles: effects on mechanical, fatigue and absorption properties, J. Mech. Behav. Biomed. Mater. 29 (2014) 451–461.
[20] D.O. O'Connor, D.W. Burke, M. Jasty, R.C. Sedlacek, W.H. Harris, In vitro measurement of strain in the bone cement surrounding the femoral component of total hip replacements during simulated gait and stair-climbing, J. Orthop. Res. 14 (1996) 769–777.
[21] A.S.T.M. International, Standard Test Method for Transition Temperatures and Enthalpies of Fusion and Crystallization of Polymers by Differential Scanning Calorimetry, ASTM International, West Conshohocken, PA, 2012.
[22] W.E. Rose, P.T. Poppens, Impact of biofilm on the in vitro activity of vancomycin alone and in combination with tigecycline and rifampicin against *Staphylococcus aureus*, J. Antimicrob. Chemother. 63 (2009) 485–488.
[23] G. Sakoulas, H.S. Gold, R.A. Cohen, L. Venkataraman, R.C. Moellering, G.M. Eliopoulos, Effects of prolonged vancomycin administration on methicillin-resistant *Staphylococcus aureus* (MRSA) in a patient with recurrent bacteraemia, J. Antimicrob. Chemother. 57 (2006) 699–704.
[24] International Organization for Standardization, Implants for Surgery — Acrylic Resin Cements, ISO, Geneva, Switzerland, 2002.
[25] A. Eitan, F.T. Fisher, R. Andrews, L.C. Brinson, L.S. Schadler, Reinforcement mechanisms in MWCNT-filled polycarbonate, Compos. Sci. Technol. 66 (2006) 1162–1173.
[26] H.W. Buchholz, H. Engelbrecht, Über die depot wirkung einiger antibiotica bei vermischung mit dem kunstharz Palacos, Chirurg 41 (1970) 511–515.
[27] M.D. Ries, Vancomycin-resistant *Enterococcus* infected total knee arthroplasty, J. Arthroplast. 16 (2001) 802–805.
[28] P. Anguita-Alonso, A.D. Hanssen, D.R. Osmon, A. Trampuz, J.M. Steckelberg, R. Patel, High rate of aminoglycoside resistance among staphylococci causing prosthetic joint infection, Clin. Orthop. Relat. Res. 439 (2005) 43–47.
[29] P.S. Corona, L. Espinal, D. Rodriguez-Pardo, C. Pigrau, N. Larrosa, X. Flores, Antibiotic susceptibility in gram-positive chronic joint arthroplasty infections: increased aminoglycoside resistance rate in patients with prior aminoglycoside-impregnated cement spacer use, J. Arthroplast. 29 (8) (2014) 1617–1621.
[30] S. Pal, Y.K. Tak, J.M. Song, Does the antibacterial activity of silver nanoparticles depend on the shape of the nanoparticle? A study of the Gram-negative bacterium Escherichia coli, Appl. Environ. Microbiol. 73 (2007) 1712–1720.
[31] C.R. Arciola, D. Campoccia, P. Speziale, L. Montanaro, J.W. Costerton, Biofilm formation in *Staphylococcus* implant infections. A review of molecular mechanisms and implications for biofilm-resistant materials, Biomaterials 33 (2012) 5967–5982.
[32] H. Ceri, M.E. Olson, C. Stremick, R.R. Read, D. Morck, A. Buret, The Calgary Biofilm Device: new technology for rapid determination of antibiotic susceptibilities of bacterial biofilms, J. Clin. Microbiol. 37 (1999) 1771–1776.
[33] S. Deresinski, Vancomycin heteroresistance and methicillin-resistant *Staphylococcus aureus*, J. Infect. Dis. 199 (2009) 605–609.
[34] B.P. Howden, J.K. Davies, P.D. Johnson, T.P. Stinear, M.L. Grayson, Reduced vancomycin susceptibility in *Staphylococcus aureus*, including vancomycin-intermediate and heterogeneous vancomycin-intermediate strains: resistance mechanisms, laboratory detection, and clinical implications, Clin. Microbiol. Rev. 23 (2010) 99–139.
[35] R.A. Proctor, C. von Eiff, B.C. Kahl, K. Becker, P. McNamara, M. Herrmann, et al., Small colony variants: a pathogenic form of bacteria that facilitates persistent and recurrent infections, Nat. Rev. Microbiol. 4 (2006) 295–305.
[36] J.A. Spadaro, D.A. Webster, R.O. Becker, Silver polymethyl methacrylate antibacterial bone cement, Clin. Orthop. Relat. Res. 143 (1979) 266–270.
[37] D.R. Monteiro, L.F. Gorup, A.S. Takamiya, A.C. Ruvollo-Filho, E.R. de Camargo, D.B. Barbosa, The growing importance of materials that prevent microbial adhesion: antimicrobial effect of medical devices containing silver, Int. J. Antimicrob. Agents 34 (2009) 103–110.
[38] E. Sudmann, H. Vik, M. Rait, K. Todnem, K.J. Andersen, K. Julsham, et al., Systemic and local silver accumulation after total hip replacement using silver-impregnated bone cement, Med. Prog. Technol. 20 (1994) 179–184.
[39] M. Nottrott, A.O. Molster, N.R. Gjerdet, Time dependent mechanical properties of bone cement. An in vitro study over one year, J. Biomed. Mater. Res. 83 (2007) 416–421.
[40] F. Tuba, V.M. Khumalo, J. Karger-Kocsis, Essential work of fracture of poly(ϵ-caprolactone)/boehmite alumina nanocomposites: effect of surface coating, J. Appl. Polym. Sci. 129 (2013) 2950–2958.
[41] R. De Santis, F. Mollica, L. Ambrosio, L. Nicolais, D. Ronca, Dynamic mechanical behavior of PMMA based bone cements in wet environment, J. Mater. Sci. 14 (2003) 583–594.
[42] H. Barani, Antibacterial continuous nanofibrous hybrid yarn through in situ synthesis of silver nanoparticles: preparation and characterization, Mater. Sci. Eng. C 43 (2014) 50–57.
[43] H. Barani, Surface activation of cotton fiber by seeding silver nanoparticles and in situ synthesizing ZnO nanoparticles, New J. Chem. 38 (2014) 4365–4370.
[44] P. Spierings, Bone cements — are they different? in: G.H. Walenkamp (Ed.), Local Antibiotics in Arthroplasty: State of the Art From an Interdisciplinary Point of View, Stuttgart: Thieme, 2007, pp. 31–39.
[45] G. Lewis, Fatigue testing and performance of acrylic bone-cement materials: state-of-the-art review, J. Biomed. Mater. Res. 66 (2003) 457–486.